

# The $W_L W_L$ scattering at the LHC: improving the selection criteria

Krzysztof Doroba<sup>a</sup>, Jan Kalinowski<sup>a,b</sup>, Jakub Kuczmarowski<sup>a</sup>,  
 Stefan Pokorski<sup>a</sup>, Janusz Rosiek<sup>a</sup>, Michał Szleper<sup>c</sup>,  
 Sławomir Tkaczyk<sup>d</sup>

<sup>a</sup>*Physics Department, University of Warsaw, Hoża 69, 00-681 Warsaw, Poland*

<sup>b</sup>*University of Hamburg, Luruper Chaussee 149, D-22761 Hamburg, Germany,  
 DESY, Notkestrasse 85, D-22607 Hamburg, Germany*

<sup>c</sup>*National Center for Nuclear Research, High Energy Physics Department,  
 Hoża 69, 00-681, Warszawa, Poland*

<sup>d</sup>*Fermi National Accelerator Laboratory, Batavia, IL 60510, USA*

May 23, 2018

## Abstract

We present a systematic study of the different mechanisms leading to  $WW$  pair production at the LHC, both in the same-sign and opposite-sign channels, and we emphasize that the former offers much better potential for investigating non-resonant  $W_L W_L$  scattering. We propose a new kinematic variable to isolate the  $W_L W_L$  scattering component in same-sign  $WW$  production at the LHC. Focusing on purely leptonic  $W$  decay channels, we show that it considerably improves the LHC capabilities to shed light on the electroweak symmetry breaking mechanism after collecting  $100 fb^{-1}$  of data at  $\sqrt{s} = 14$  TeV. The new variable is less effective in the opposite-sign  $WW$  channel due to different background composition.

## 1 Introduction

The longitudinal  $WW$  scattering carries the most direct information about the mechanism of electroweak symmetry breaking, no matter whether a physical elementary Higgs particle exists or some kind of strongly interacting physics is responsible for this breaking. In fact, even if a light Higgs boson is discovered, the energy dependence of the longitudinal  $WW$  scattering above the Higgs mass scale will tell us if the Higgs boson unitarizes the  $WW$  scattering fully or only partially, as in some theoretical models with composite Higgs [1]. Experimental investigation of the  $W_L W_L$  scattering as a function of its center-of-mass energy  $M_{WW}$  becomes feasible at the LHC. The techniques for observing the  $W_L W_L$  scattering signal in  $pp$  collisions have been extensively investigated and reported

in many papers ([2]–[11]). They are based on the differences in the emission process of the transverse and longitudinal gauge bosons from the colliding quarks and in the behavior of the  $WW$  scattering amplitudes as a function of their center-of-mass energy and the scattering angle. Those effects are, however, strongly masked by the quark distribution functions inside the proton and by various sources of large background. It has been found that such techniques as forward jet tagging, central jet vetoing, and cuts on the final lepton transverse momenta are very promising in the isolation of the  $W_LW_L$  scattering signal from the background. At the same time, the above studies clearly showed that such measurement would be experimentally very challenging and typically require from more than a year to several years of LHC running at full nominal parameters to obtain observable effects. In view of this, a deeper understanding of the process on the theoretical side and possible new techniques allowing for a better event selection and a better data analysis can play an important role to make the study feasible in a relatively shorter timescale.

Given the importance of the experimental access to the longitudinal  $WW$  scattering channel, we readdress this issue in the present paper. We analyze the feasibility of observing the signal of an enhanced, compared to the prediction of the SM with a light Higgs boson,  $W_LW_L$  scattering at the LHC running at an energy of 7, 8 and 14 TeV. As our laboratory for the enhanced  $W_LW_L$  scattering we use the higgsless scenario. If a Higgs boson does exist, but with couplings modified compared to the SM so that it does not fully unitarize the  $WW$  scattering, the signal will be weaker and more difficult to observe (see e.g. [12]).

In search for the most efficient event selection criteria, we first present a systematic study of the different mechanisms leading to  $WW$  pair production at the LHC, both in the same-sign and opposite-sign channels. We justify why and under which conditions the complicated process of  $WW$  production in  $pp$  collisions can be reduced to general considerations on  $W_L$  and  $W_T$  emission off a quark line. We then examine the differences between emission and scattering processes of the  $W$  bosons of well defined, longitudinal or transverse polarizations. For quantitative analyses we apply exact matrix element calculations involving the MADGRAPH generator [13]. We also briefly show that some basic features of  $W$  emission can be qualitatively understood within the framework of the Effective  $W$  Approximation (EWA) [14].

Based on our study, we propose a new kinematic variable for the longitudinal  $W^+W^+$  scattering signal, showing that it gives significant improvement of the signal-to-background ( $S/B$ ) figures compared to all the previously discussed selection criteria. We furthermore emphasize that  $WW$  scattering with same-sign  $W$ 's offers the best physics potential for the LHC.

In this work, we choose to focus on the purely leptonic  $W$  decays in both the same-sign and opposite-sign  $WW$  scattering processes. These channels are known as “gold plated”, in spite of their low statistics, for their relatively low background contaminations and experimental purity.

## 2 Signal and background definitions

Following the well established “subtraction method” [2], we define the signal as the enhancement in the production of  $WW$  pairs in association with two parton jets in the higgsless scenario over the prediction of the Standard Model with a 120 GeV Higgs:

$$\text{Signal} = \sigma(pp \rightarrow jjWW)|_{\text{higgsless}} - \sigma(pp \rightarrow jjWW)|_{M_h=120\text{GeV}}. \quad (1)$$

It is worth to note that even an observation of a light Higgs boson does not necessarily exclude a non-vanishing signal, assuming that it may have non-standard couplings to vector bosons. The signal comes on top of the irreducible background, which is:

$$\text{Background} = \sigma(pp \rightarrow jjWW)|_{M_h=120\text{GeV}}. \quad (2)$$

For the calculations in the higgsless scenario, we make no distinction between removing all Feynman diagrams involving Higgs exchange or setting an inaccessibly large Higgs mass ( $10^{10}$  GeV) in the calculation. Furthermore, instead of using any particular unitarization model, we will assume the  $W_L W_L$  scattering cross section saturates just before its partial wave amplitudes hit the perturbative unitarity limit at a  $WW$  center of mass energy around 1.2 TeV and stays constant above this value. Such assumption defines the practical limiting case for a signal size which is still consistent with all physics principles. Once all the appropriate selection criteria are applied, we find this prescription reduce the signal size by 20-23%, depending on the selection details, compared to the purely mathematical higgsless case with no unitarization at all (of course, mostly affected is the most interesting region of large invariant  $WW$  masses).

To a good approximation, the signal comes from the scattering of longitudinally polarized  $W$  bosons, by far the most sensitive to the electroweak symmetry breaking dynamics. Irreducible background is dominated by the transverse  $W$  production.

The cross sections appearing in the definition of the signal and the background must be calculated in a gauge invariant way, including also  $O(\alpha^2)$  (pure EW) and  $O(\alpha\alpha_S)$  (QCD) diagrams in which two  $W$ 's are produced but do not interact. As we shall discuss below, QCD effects in particular play an important role in the correct calculation of the background.

Both for the signal and for the background we perform a full matrix element calculation of the processes  $pp \rightarrow jjW^+W^+$  and  $pp \rightarrow jjW^+W^-$  using the MADGRAPH generator, followed by leptonic  $W$  decay and quark hadronization. The procedure implies that the intermediate state  $W$ 's are on-shell, which in literature is sometimes referred to as the “production  $\times$  decay” approximation. In particular, diagrams which contribute to the same final state but do not proceed via an intermediate state consisting of a  $WW$  pair are here neglected. The  $W$  decay is simulated using a private version of PYTHIA 6 which has the appropriate angular distributions for the decays of  $W_L$  and  $W_T$  implemented. Such modification of the code (in the standard distribution of PYTHIA 6 [15] the  $W$ 's are decayed isotropically) is vital in order to obtain the correct kinematic distributions of the final state leptons. To check the validity of the  $W$  on-shell approximation, a dedicated study was carried out, in which special samples of the  $pp \rightarrow jjW^+W^+ \rightarrow jjl^+l^+\nu\nu$  process generated using this method were compared in detail with  $pp \rightarrow jjl^+l^+\nu\nu$  samples

generated with the PHANTOM program [16], without resorting to any “production  $\times$  decay” approximation<sup>1</sup>. After imposing exactly the same generation cuts on both samples, comparisons of the respective kinematic distributions of the final state leptons do not reveal large differences, as shown in Fig. 1. An overall uncertainty in the normalization amounting to a few per cent is apparent for the EW background, but all lepton kinematics is adequately described. The signal calculated in the  $W$  on-shell approximation reveals a deficit of events at low invariant masses of the  $l^+l^+$  pair ( $M_{ll} < 200$  GeV). However, this kinematic region is of little relevance for the present analysis and, as we will see later, will be almost completely eliminated by the selection criteria. We conclude that the “production  $\times$  decay” approximation is unlikely to be a source of any significant bias in the results.

We have also cross checked our calculations for the pure EW  $jjW^+W^-$  production against the numbers from Table 7 of Ref. [7] that were calculated using VBFNLO and including NLO QCD corrections to the purely electroweak tree-level process. At the level of their “inclusive” cuts, for both Higgs boson mass hypotheses of 100 GeV and 1 TeV, we find satisfactory agreement, although the agreement in the total cross section expectedly breaks down in the Higgs resonance region.

In the “production  $\times$  decay” approximation, the signal and the background can be calculated as respective sums over different polarizations of the final  $WW$  pairs. The dependence of the transverse and mixed transverse-longitudinal  $WW$  pair production on the Higgs boson mass, up to the higgsless limit, is weaker than 3% overall. Although it is a part of the signal in the sense of Eq. (1) (and not necessarily negligible given  $W_LW_L$  overall smallness), this contribution has no specific kinematic signature that would allow to isolate it from the much larger background. In the kinematic range where  $WW$  scattering can be observed and background sufficiently suppressed it becomes completely negligible and will be ignored further on.

Thus, our effective technical definitions of signal and background can be rewritten as:

$$\text{Signal} = \sigma(pp \rightarrow jjW_LW_L)|_{\text{higgsless}} - \sigma(pp \rightarrow jjW_LW_L)|_{M_h=120\text{GeV}}, \quad (3)$$

$$\text{Background} = \sigma(pp \rightarrow jjW_LW_L)|_{M_h=120\text{GeV}} + \sigma(pp \rightarrow jjW_TW_T) + \sigma(pp \rightarrow jjW_TW_L), \quad (4)$$

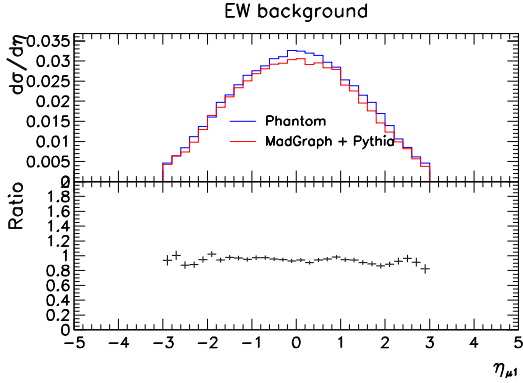
where each polarization cross section is given in the most general case by a sum of interfering amplitudes: pure electroweak diagrams with interacting and non-interacting  $WW$  pairs and QCD-electroweak diagrams with non-interacting  $WW$  pairs.

### 3 $W$ pair production at the LHC. Emission and scattering of longitudinal and transverse $W$ 's

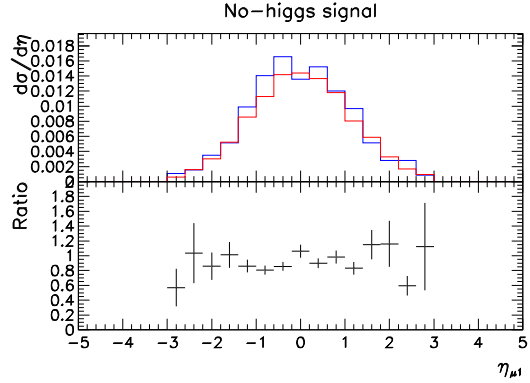
Production of  $WW$  pairs with two associated parton-level jets at the LHC involves hundreds of tree-level diagrams and in general is dominated by events with no direct relevance to the mechanism of electroweak symmetry breaking. Signal selection can be crudely divided into two steps: “basic” cuts suppressing the soft parton-parton collisions (both

---

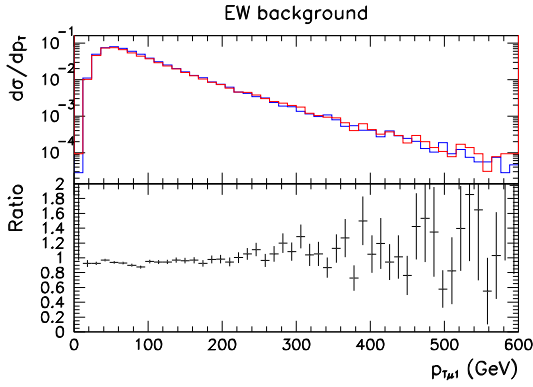
<sup>1</sup>MS is grateful to the authors of Ref. [11] for granting him access to the PHANTOM data samples.



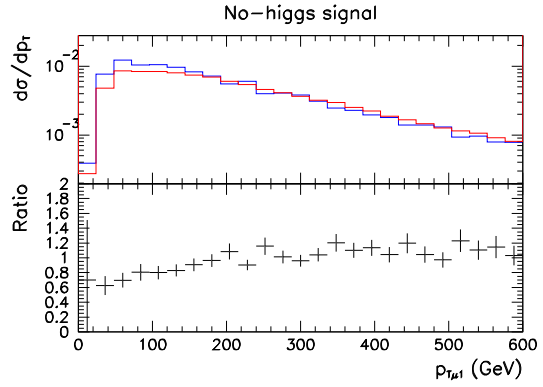
a)



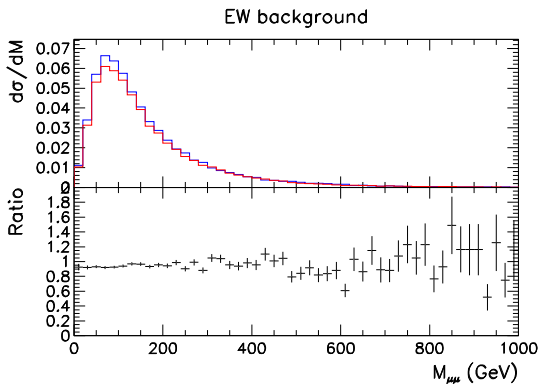
b)



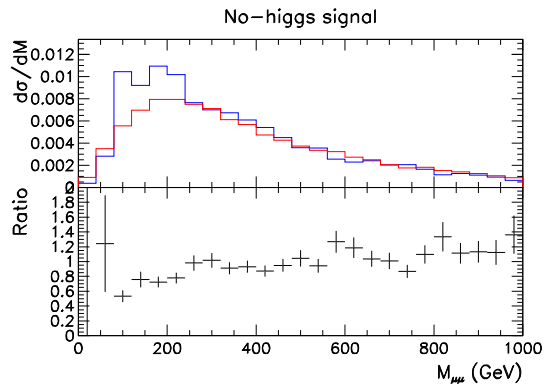
c)



d)



e)



f)

Figure 1: Kinematic distributions of final state muons from the  $pp \rightarrow jj\mu^+\mu^+\nu\nu$  process at 14 TeV, obtained using the  $W$  on-shell approximation (labeled MadGraph+Pythia) and exact matrix element calculations (labeled Phantom). Pseudorapidities (a,b), transverse momenta (c,d) and invariant masses (e,f) are shown. For the sake of comparison, background samples contain pure EW processes only and a 200 GeV Higgs is assumed.

QCD and EW related) and leaving mostly the events with hard  $W$  interactions, then “final” cuts distinguishing the  $W_L W_L$  scattering from the irreducible background mainly from  $W_T W_T$  and  $W_T W_L$  pairs.

The  $WW$  production cross section with polarized  $W$ 's in the final state can schematically be written as follows:

$$d\sigma_{ij}(M, m_h) = |a(M, m_h)_{ij}\alpha^2 + b(M)_{ij}\alpha\alpha_s|^2 \quad (5)$$

where  $M$  is the invariant mass of the  $WW$  pair,  $m_h$  is either 120 GeV or denotes the higgsless case,  $\alpha$  ( $\alpha_s$ ) is the electroweak (strong) coupling squared and subscripts  $i$  and  $j$  denote the final  $W$  pair polarizations. At the production amplitude level the  $a$  term sums all the pure EW contributions and the  $b$  term comes from a mixed EW/QCD process which is  $m_h$  independent. From the above schematic formula the signal defined in Eq. (3) can be written as

$$\begin{aligned} \text{Signal} &\propto \alpha^4 \left[ |a(M, \text{higgsless})_{LL}|^2 - |a(M, m_h = 120)_{LL}|^2 \right] \\ &+ 2\alpha_s^2 \alpha^2 \text{Re} \left[ (a(M, \text{higgsless})_{LL} - a(M, m_h = 120)_{LL}) b^*(M)_{LL} \right] \end{aligned} \quad (6)$$

From the above one sees that the signal is driven by pure EW processes. The large term  $|b_{LL}|^2$  cancels out in the difference through which we define the signal. Moreover, as shown

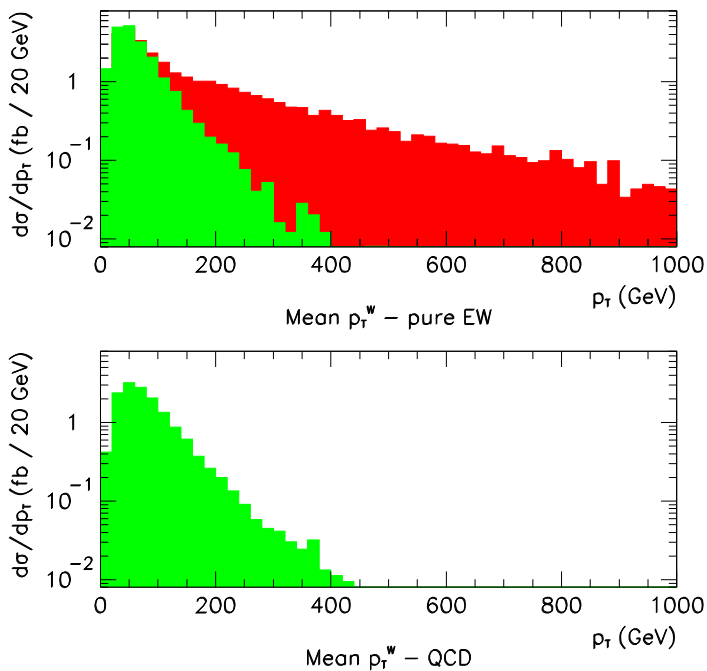


Figure 2: Transverse momentum distributions of the  $W$  coming from pure EW production (top) and from QCD production (bottom). Electroweak signal, in the sense of Eq. (3), is shown in red (dark grey). Shown in green (light grey) are contributions to the background.

in Fig. 2, QCD events populate mostly a different region of kinematic phase space than the electroweak signal events (mostly apparent in the respective distributions of the  $W$  transverse momenta), so interference terms described by the product  $[a(p_T^W, \text{higgsless})_{LL} - a(p_T^W, m_h = 120)_{LL}] \cdot b^*(p_T^W)_{LL}$  also remain negligibly small compared to the pure EW contribution. This conclusion is valid as much for  $W^+W^+$  as for  $W^+W^-$ , even though in the latter case QCD processes dominate the total production rates.

For background that includes also  $WW$  bosons with  $ij = LT, TT$  polarizations, the effect of QCD processes is much more important since  $|b_{ij}|^2$  term is present, and the coherent sum  $a_{ij}\alpha$  does not overwhelm  $b_{ij}\alpha_s$ . In fact, QCD contributions to the total  $jjW^+W^-$  production dominate the total cross section by roughly an order of magnitude. In particular, processes involving quark-gluon and gluon-gluon interactions, absent in the same-sign  $WW$  channel, here amount to as much as 60% of the total  $W^+W^-$  production cross section. For the same-sign  $WW$  production, only quark-quark interactions can contribute and QCD effects, in form of diagrams involving gluon exchange, amount to roughly 50% of the total cross section. Most of these events originate from soft parton-parton collisions (soft partons dominate in the proton PDFs), give very soft kinematics of the accompanying parton jets and can be rejected by appropriate cuts on their rapidity.

Conventional selection criteria for  $WW$  scattering processes include the requirement of two tag jets in the forward region and in opposite directions. We will quantify this requirement as

$$2 < |\eta_j| < 5 \quad \text{and} \quad \eta_{j1} \cdot \eta_{j2} < 0. \quad (7)$$

where the  $\eta_j$  denote pseudorapidities of the parton-level jets. Detector acceptance imposes stringent limits on the allowed lepton kinematics to be considered, which at the level of undecayed  $W$  can be approximated as a cut on the  $W$  pseudorapidity,

$$|\eta_W| < 2. \quad (8)$$

The effect of these basic cuts is twofold. As illustrated in Fig. 3, they significantly reduce the irreducible electroweak background coming from low energy parton-parton collisions, that is in the region of small transverse momenta of the parton-level jets. They also reduce the QCD background, to the effect of same-sign  $WW$  production being dominated by pure electroweak production.

Ultimately, a full calculation of the same-sign  $WW$  production with all the proper EW/QCD interference terms included ends up in background rates that are larger by less than 10% compared to a pure EW calculation after all selection criteria are applied and indeed, many previous studies neglected this contribution altogether. However, the residual QCD contribution to the background in the  $W^+W^-$  channel is still sizable, including that from quark-gluon and gluon-gluon interactions and from other processes which change the overall kinematic characteristic of the background for  $W^+W^-$ .

In all our MADGRAPH calculations we use a fixed factorization and renormalization scale of 91.188 GeV. Our QCD cross sections for the process  $pp \rightarrow jjW^+W^-$  are in agreement to  $\sim 10\%$  with the respective numbers from Table 7 of Ref. [7] once their “inclusive” cuts are applied, which may well be taken as the intrinsic uncertainty of our QCD background calculations. It should be noted however that unlike the authors of Ref. [7] we compute QCD backgrounds together with EW backgrounds, with all due interference terms in place.

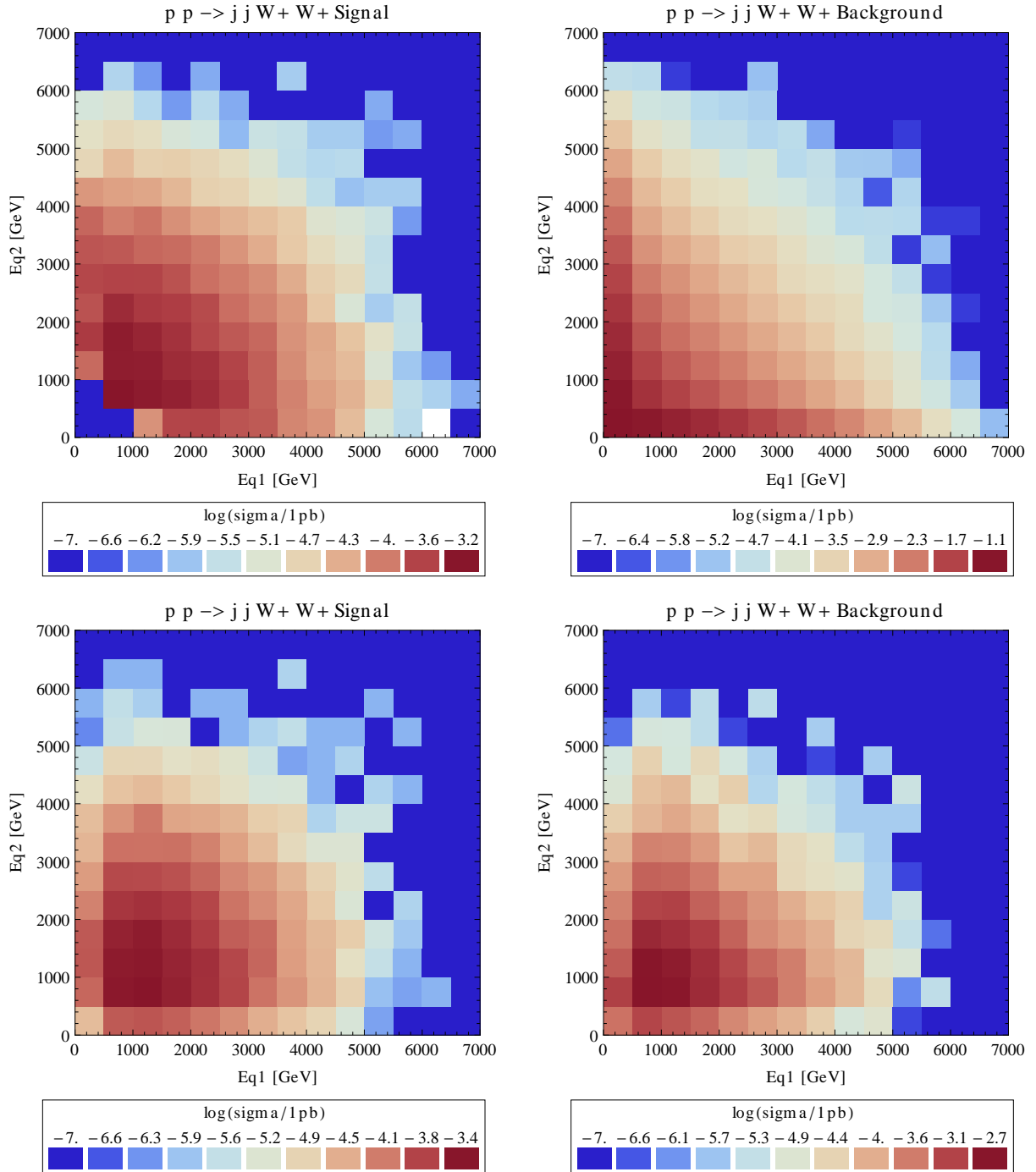


Figure 3: Cross section for the  $pp \rightarrow jjW^+W^+$  process at 14 TeV as a function of incident quark energies. Left column: signal as defined in Eq. (3), right column: background (Eq. (4)), upper row: without cuts, lower row: after "basic" cuts of Eqs. (7,8).



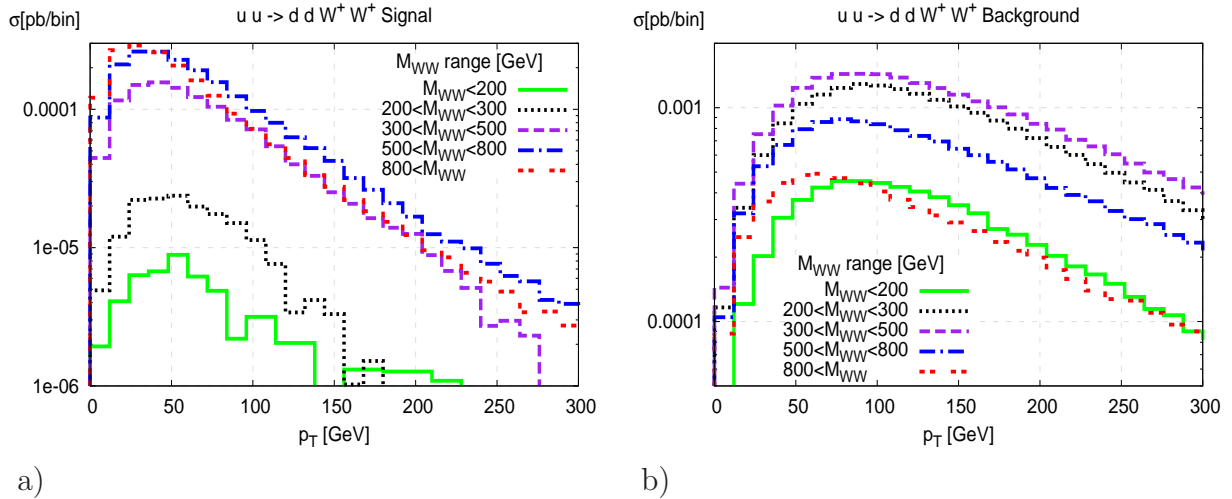


Figure 4:  $p_T$  distributions of parton-level jets in symmetric quark-quark collisions  $uu \rightarrow jjW^+W^+$  with initial quarks of 1 TeV energy: (a) signal, (b) background. Results from a MADGRAPH calculation.

From Fig. 3 we see that basic cuts on the pseudorapidities of parton-level jets and the outgoing  $W$ 's in the same-sign channel case produce a sample of events with little contamination from low energy quark-quark collisions. For the background this also means little QCD contribution left. At the quark level, the process that dominates same-sign  $WW$  production at the LHC is an approximately symmetric quark-quark interaction, with its center-of-mass energy typically peaking at  $\sim\sqrt{s}/7$ , associated with a  $W$  emission from each quark line. Thus the basic features of  $pp \rightarrow jjW^+W^+$  at 14 TeV are qualitatively similar to those of a pure quark level process  $uu \rightarrow ddW^+W^+$  at an energy of about 2 TeV. Analysis of this much simpler process is helpful in deriving effective criteria to separate the  $W_LW_L$  scattering signal from the background that remains after the “basic” cuts and includes scattering processes with transverse  $W$ 's.

The characteristic difference in the kinematics of the LL and TT+TL final states in the quark-level process are illustrated in Fig. 4 where the results of a MADGRAPH simulation of the  $uu \rightarrow ddW^+W^+$  process at 2 TeV are shown. The longitudinally polarized  $W$  tends to be emitted at a smaller angle (hence smaller  $p_T$ ) with respect to the incoming quark direction than the transversely polarized  $W$  [17, 2]. As a consequence, the final quark accompanying the longitudinal  $W$  is more forward than the one associated with the transverse  $W$ . This effect is more pronounced the larger the invariant mass of the  $WW$  pair. The  $p_T$  distributions of quarks associated with  $W_L$  emission become narrower as  $M_{WW}$  increases and the peak of the distributions gradually moves to lower values. No such trend is visible for the quarks associated with  $W_T$  emission, except for  $M_{WW}$  larger than 800 GeV, where the effects of overall energy and momentum conservation become significant.

Those qualitative observations suggest that the higher the invariant mass of the  $WW$  pair the easier becomes the isolation of the longitudinal  $WW$  signal from the transverse  $WW$  background. Tagging of forward jets at a fixed large value of  $M_{WW}$  is the ideal technique to be used.

It is interesting to note that all these features are qualitatively reproduced within the

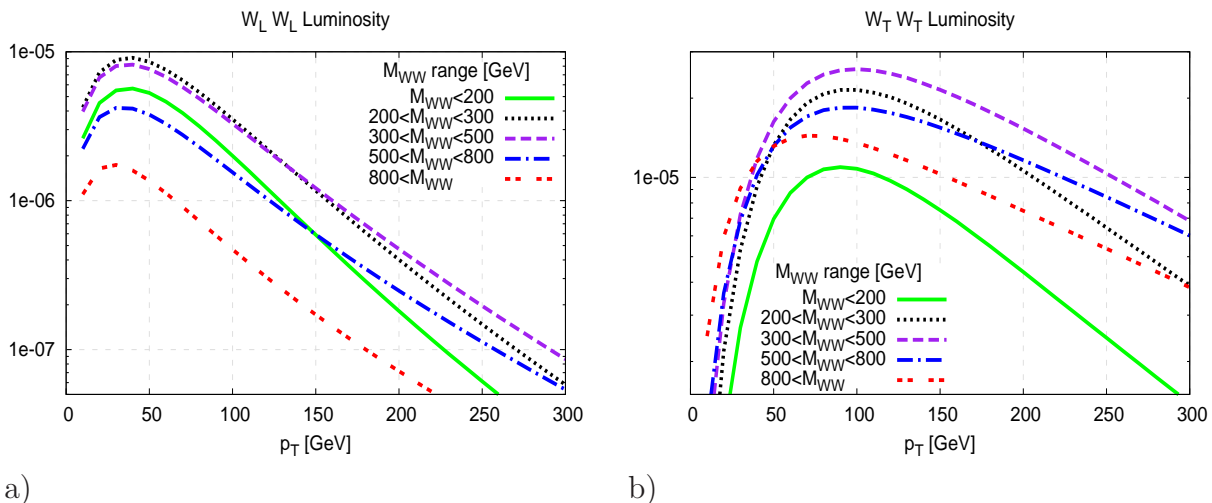


Figure 5:  $p_T$  distributions of parton-level jets associated with  $W$  emission in symmetric quark-quark collisions with initial quarks of 1 TeV energy: (a) for longitudinal  $W$ 's, (b) for transverse  $W$ 's. Result (up to an overall normalization factor) of an EWA calculation of the emission probability of two  $W$ 's, each from a different quark line, for given  $W$  helicities and  $WW$  invariant mass ranges.

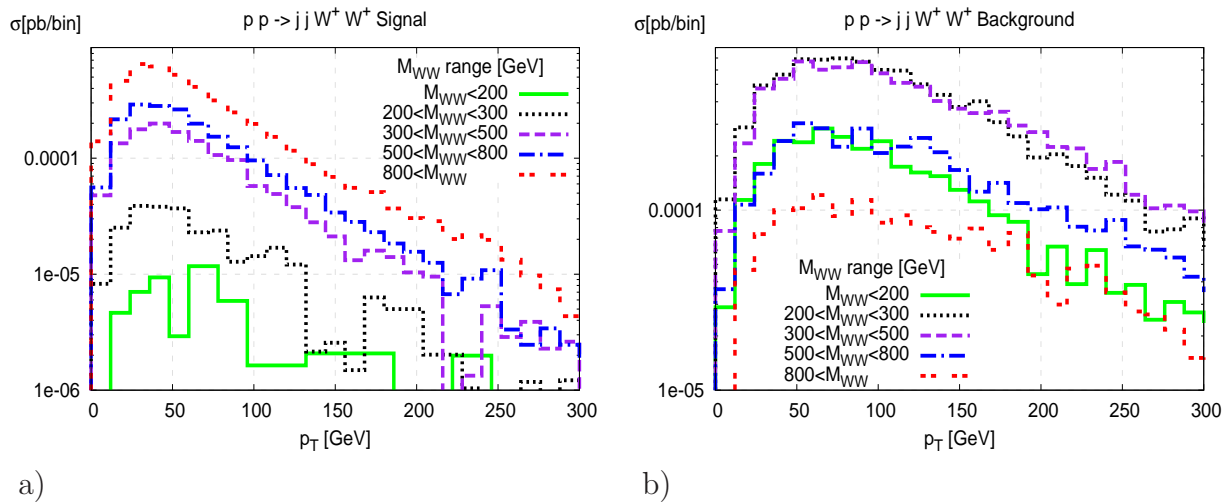


Figure 6:  $p_T$  distributions of jets in a proton-proton collision  $pp \rightarrow jjW^+W^+$  with each proton of 7 TeV energy: (a) signal, (b) background, after applying the basic cuts described in the text. Results of a MADGRAPH calculation.

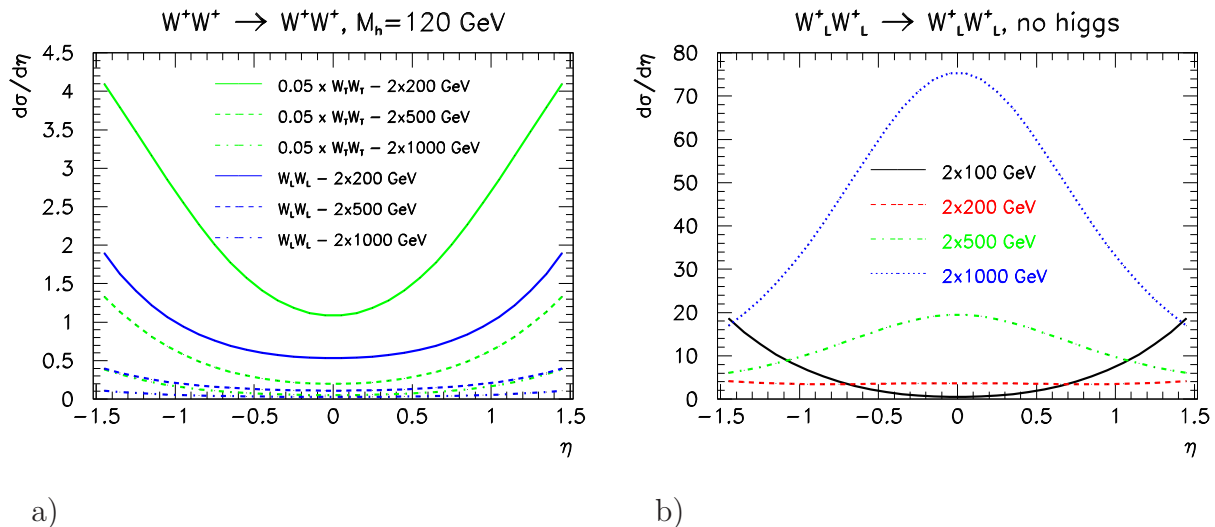


Figure 7: Angular distributions of scattered  $W$ 's with respect to the incoming  $W$  direction, in a  $W^+W^+$  scattering process at different center of mass energies: (a) in the presence of a 120 GeV Higgs boson, (b) in the no-Higgs case.

framework of the Effective  $W$  Approximation, where we can identify the signal and the background with  $W_L W_L$  and  $W_T W_T$ , respectively (Fig. 5).

In  $pp$  collisions, the above regularities are at first completely masked by the overwhelming low energy and highly asymmetric quark-quark collisions as well as QCD effects, but become visible again after the basic cuts discussed earlier. This is shown in Fig. 6.

The bounds on  $\eta_W$  (here mimicking cuts on the pseudorapidities of  $W$  decay products that are necessary to meet detector acceptance criteria) are instrumental in further reduction of the  $TT+TL$  background. As shown in Fig. 7, in an ideal process  $WW \rightarrow WW$ , with two beams of real  $W$ 's colliding at a fixed energy  $M_{WW}$ , the angular distributions of the scattered longitudinal and transverse  $W$ 's (measured in the  $WW$  center of mass and with respect to the incoming  $W$  direction) become more different with the increase of  $M_{WW}$ . The cross sections for  $WW$  scattering with polarization flip, e.g.  $W_T W_T \rightarrow W_L W_L$ , are typically three orders of magnitude smaller than the polarization-conserving ones and cannot influence the overall angular characteristics.

As discussed above, jet  $p_T$  distributions depend on the emitted  $W$  polarization and in particular  $W_T$  rejection can be improved by requiring smallness of the transverse momenta of both jets. Any higgsless or non-SM Higgs scenario will modify the angular distributions of outgoing longitudinal  $W$ 's by making them more central with respect to the incoming  $W_L$  direction. Requirement of a large vector boson  $p_T$  measured in the lab frame combines the effects of a large  $W$  scattering angle and small  $W$  emission angle from the parent quark line, both of which favor longitudinal over transverse  $W$ 's. In search for the most efficient selection criterion that would combine low jet  $p_T$  and large vector boson  $p_T$ , we notice that in the small  $|\eta_W|$  region the  $M_{WW}$  value strongly correlates with the product of the two transverse momenta,  $p_T^{W1} \cdot p_T^{W2}$ . In the leptonic  $W$  decay channels, where we do not know the exact kinematics of the two decaying  $W$ 's, the  $p_T$  values of the leptons and in particular their product are the best practical measures of  $M_{WW}$ . Consequently, a large value of the

product  $p_T^{l_1} \cdot p_T^{l_2}$  is an approximate experimental signature of the kinematic region which is most sensitive to the actual mechanism of electroweak symmetry breaking and offers the best capabilities to separate longitudinal from transverse  $WW$  scattering processes in any scenario that enhances the  $W_L W_L$  cross section for large  $M_{WW}$ . Correlation between high  $p_T^{l_1} \cdot p_T^{l_2}$  and high  $M_{WW}$  is stronger if one additionally asks for large ratios of  $p_T^l/p_T^j$ . For high pseudorapidity jets this means removing events with very large jet energies and little energy left for the  $W$ .

The above considerations make it clear that a large value of the following ratio  $R_{p_T}$  of the four transverse momenta:

$$R_{p_T} = \frac{p_T^{l_1} \cdot p_T^{l_2}}{p_T^{j_1} \cdot p_T^{j_2}}, \quad (9)$$

where  $l_1$  and  $l_2$  denote the two leptons in no particular order and  $j_1$  and  $j_2$  denote the two most energetic jets in the event, is bound to have a large efficiency in isolating hard  $W_L W_L$  scattering from the SM background. Such ratio automatically accounts for the correlations that are likely to be satisfied by the signal, but not by the background, and thus work more efficiently than a collection of uncorrelated cuts on the individual variables.

In the rest of the paper we discuss the impact of using the new variable as a selection criterion and the resulting perspectives for the observation of  $W_L W_L$  scattering at the LHC. In particular, in Section 5 we compare the selection efficiencies with and without the variable  $R_{p_T}$  in the analysis of the same-sign  $WW$  channel and demonstrate that the new criterion can significantly improve the  $S/B$  figures for this process.

The kinematics of signal and background for the opposite-sign channel differs from that of the same-sign channel in several significant ways. Apart from the residual QCD background which softens the average jet  $p_T$  and worsens its separation from the signal, pure EW background receives additional contributions from  $t$ -channel processes in which both the  $W^+$  and the  $W^-$  originate from the same parent quark line. This is another source of softening of the average jet  $p_T$  for jets accompanying  $W_T^+ W_T^-$  pairs and a class of processes not covered in the EWA approach. On top of that, both signal and background receive contributions from  $s$ -channel processes with a  $W^+ W^-$  pair being produced from a  $Z$  or a Higgs boson. Finally, parton distribution functions also play some role, since the two valence  $u$  quarks of the proton favor  $W^+ W^+$  production. All these effects change the overall kinematics of the signal and, most importantly, of the irreducible background. In Section 6 we show that these features indeed reduce the practical usefulness of the  $R_{p_T}$  variable in the analysis of the opposite-sign channel.

## 4 Reducible background

Among the many potential sources of reducible background, inclusive  $t\bar{t}$  production appears to be most difficult to suppress. Having this background under control is of course most critical in the  $jjW^+W^-$  channel where top decays can directly fake the signal. It turns out however that also in the  $jjW^+W^+$  channel, due to the huge initial cross section for  $t\bar{t}$  production, even tiny detector effects cannot be completely disregarded and can contaminate the signal to measurable amounts, necessary to estimate and subtract. The

two main mechanisms for a  $t\bar{t}$  pair to fake the same-sign  $WW$  scattering signal are: lepton sign misidentification and leptonic  $B$  decays.

We have developed and implemented two independent methods to estimate the magnitude of the inclusive top pair production. The first method relies on an analysis of two separate samples generated with MADGRAPH: one of  $pp \rightarrow t\bar{t}$  and another of  $pp \rightarrow t\bar{t}q$  (top pair production with an associated light quark). Both samples were then processed with PYTHIA to account for the effects of initial and final state radiation, top decay, hadronization and jet formation. Since the respective sets of Feynman diagrams which are included in the calculation of the two samples are mutually exclusive, the procedure does not involve any event double counting and the events can be simply added at the end. The caveat of this method is that it does not encompass all possible processes leading to top pair production with one or two additional jets, since diagrams involving gluon emission off an internal quark line are neglected here. However, our cross section calculation for  $\sqrt{s} = 7$  TeV gives a total of 198 pb, which is in fair agreement with already published CMS and ATLAS data [18].

In the second method we generate three samples using MADGRAPH:  $pp \rightarrow t\bar{t}$ ,  $pp \rightarrow t\bar{t}j$  and  $pp \rightarrow t\bar{t}jj$ , with  $j = q, g$ , then we likewise use PYTHIA for initial and final state radiation, top decay, hadronization and jet formation. To avoid double counting of the events we follow the prescription described in more detail in Ref. [7], which amounts to selecting from each sample only the events with mutually exclusive topologies. In our case, we keep only events in which the number of  $b$  quarks outgoing at a pseudorapidity  $2 < |\eta| < 5$  is 2, 1 or 0, respectively. The three samples thus represent the respective lowest order processes for which 0, 1 or 2 tagging jets arise from gluons or light quarks. This method is formally more complete and coherent, even though the total cross section without cuts cannot be deduced and confrontation with existing experimental data must necessarily rely on comparisons with results obtained from the former method. All the  $t\bar{t}$  numbers we will quote in this paper are to be understood as arising specifically from the latter method and having been additionally cross checked with the former.

In the determination of  $t\bar{t}$  background we will be assuming throughout this paper an average  $b$ -tagging efficiency of 50% for a single  $b$ , with a negligible ( $\sim 1\%$ ) probability of mistagging a lighter quark or gluon, in reasonable consistency with recent CMS reports [19].

Determination of background arising from leptonic  $B$  decays requires final state radiation switched on and some jet reconstruction procedure to be adopted. In this work we used the jet reconstruction algorithm which is provided by PYTHIA routine PYCELL, with the cone width set to 0.7. For consistency we also used exactly the same procedure for the irreducible background as well as for the signal. Compared to a pure parton-level analysis, this implies a decrease in the number of accepted signal events by nearly 10%.

The primary selection criteria used to suppress the  $t\bar{t}$  background consist of stringent cuts on the invariant mass of the two most energetic jets in the event and combinations of jets with leptons, see Fig. 8. Based on these distributions we chose to apply cuts on the invariant masses of combinations  $j_1l_2$  and  $j_2l_1$  (both jets and leptons are ranked according to their transverse momenta) at 200 GeV. Cuts on the other two jet-lepton combinations are optional, we find however they do not improve the final figure of merit, defined as  $S/\sqrt{S+B}$ , and hence we drop them. We also apply a cut on the jet-jet invariant mass whose actual value is subject to individual optimization in each analysis.

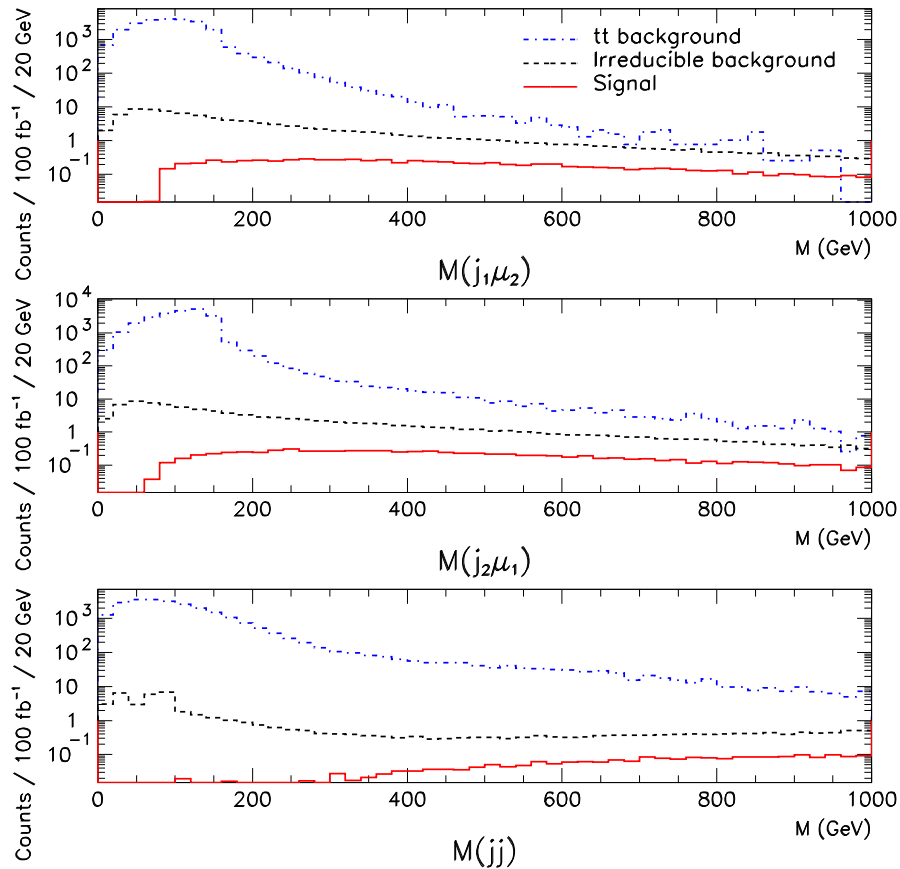


Figure 8: Kinematic distributions of the  $t\bar{t}$  background compared to signal and irreducible background in the  $pp \rightarrow jj\mu^+\mu^+\nu\nu$  process at 14 TeV: Invariant masses of two leading jets (bottom) and combinations of jets and muons (top and middle).

Furthermore, in order to estimate some reasonable event yields in the analysis of the same-sign  $WW$  channel, we will assume a realistic efficiency of muon sign matching of 99.5% for  $p_T \sim 300$  GeV [20]. For electrons at  $|\eta| < 2$ , a 99% sign matching capability with an overall electron reconstruction efficiency of 95% seems attainable in CMS [21] and these values will be assumed in the rest of the paper.

We have not studied any possible additional sources of reducible background in this work since they have been shown less relevant in both the  $jjW^+W^+$  and  $jjW^+W^-$  channels (e.g. [22]) and partly because most of these backgrounds involve various detector effects which cannot be studied without a proper detector simulation. In particular, one should be mindful of the potentially harmful additional reconstruction backgrounds in the electron channel, notably the “fake electron” background, but such considerations surpass the scope of the present work.

## 5 The same-sign $WW$ channel

We have generated the following samples:  $jjW^\pm W^\pm$  in the SM with a 120 GeV Higgs (accounting for the total irreducible background),  $jjW_L^\pm W_L^\pm$  in the SM with a 120 GeV Higgs and in the higgsless case (for the signal calculation) and several  $t\bar{t}$  samples generated as described in the previous Section. Generated numbers of events and the respective cross sections, together with other details, are shown further in Tables 1 and 2. The only generation level cut was  $2 < |\eta_j| < 5$  for both outgoing parton-level jets (except for the  $t\bar{t}$  samples, where no generation level cuts were applied), to avoid the most background dominated kinematical region and satisfy detector acceptance.

The conventional approach to decrease the irreducible background consists of applying a set of uncorrelated leptonic cuts in addition to jet cuts. As discussed in Section 3, leptons originating from the decay of hard  $WW$  scattering processes tend to have larger transverse momenta, they are more central, more back-to-back and have larger invariant masses than those from background processes. Finally, the bulk of the background from  $t\bar{t}$  with a  $B$  meson decaying into leptons can be efficiently suppressed by lepton isolation techniques which we will approximate here with a requirement of no reconstructed jets within a cone of 0.4 centered at each lepton. We also require no tagged  $b$  and no additional leptons with  $p_T > 10$  GeV within  $|\eta| < 2$ . A complete set of conventional signal selection criteria can therefore be as follows (set I):

- exactly 2 same sign leptons within detector acceptance,
- 2 tag jets with  $2 < |\eta_j| < 5$  and opposite directions,
- no  $b$ -tag,
- $M_{j_1 l_2}, M_{j_2 l_1} > 200$  GeV,
- $M_{jj} > 400$  GeV,
- $\Delta R_{jl} > 0.4$ ,
- $p_T^{l_1}, p_T^{l_2} > 40$  GeV,
- $|\eta_{l_1}|, |\eta_{l_2}| < 1.5$ ,
- $\Delta\phi_{ll} > 2.5$ ,
- $M_{ll} > 200$  GeV.

After adding all the same-sign leptonic channels together ( $l^+ = \mu^+, e^+$ ), we get selection efficiencies and final cross sections that are given in Table 1 and the  $l^+l^+$  invariant mass of the selected events is shown in Fig. 9(a). Normalized to  $100 fb^{-1}$ , we get a signal to background  $S/B \approx 11/7$ . It should be stressed here that surviving background includes a measurable amount of  $t\bar{t}$  and that its dominant source at this point is lepton sign misidentification. The inclusion of the  $W^-W^-$  channel provides an additional 25% to the signal and irreducible background (see Table 2), but at the same time the  $t\bar{t}$  background doubles, ending up in  $S/B \approx 13/11$ . The corresponding  $ll$  invariant mass distribution

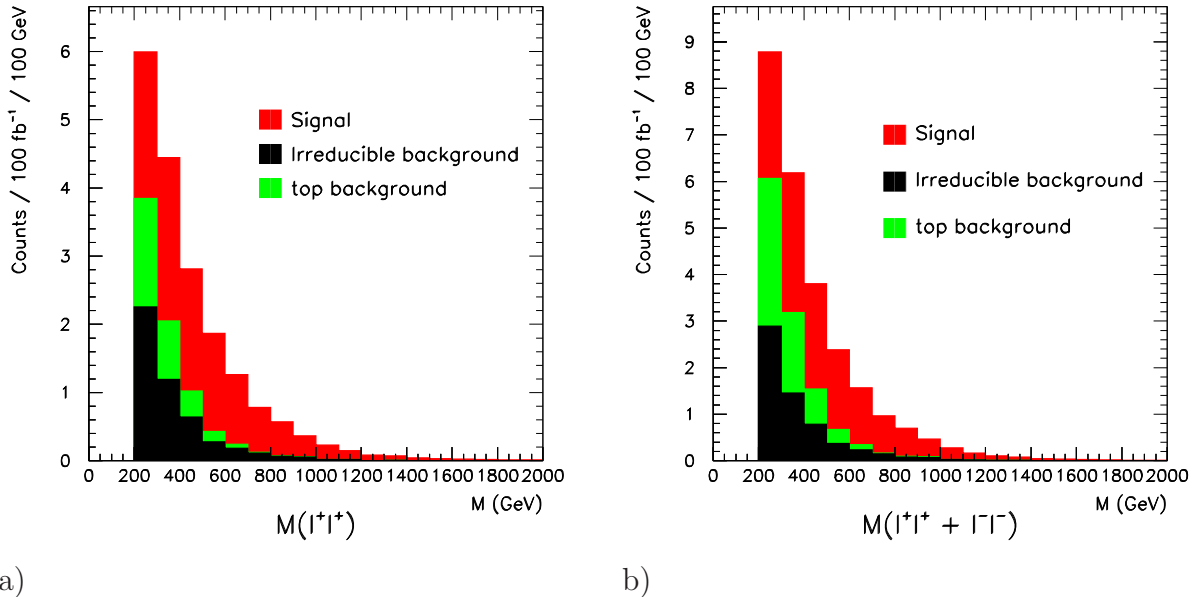


Figure 9: Invariant mass distributions of two same-sign leptons after all the conventional signal selection criteria (set I), normalized to  $100 \text{ fb}^{-1}$ : (a)  $jjl^+l^+$ , (b)  $jjl^+l^+$  and  $jjl^-l^-$  added.

is shown in Fig. 9(b). Although our set of cuts is not very fine tuned, it already allows to produce a result which is roughly comparable with previous analyses in the same-sign lepton channel, in particular with the recent Ref. [5]. Several differences exist between the two analyses (in order of relevance: no  $t\bar{t}$  background included, no unitarity limit applied in the no-Higgs case, cuts done on parton level variables, different treatment of QCD background and a different default Higgs mass). Recalculating under their assumptions, our result translates into  $S/B \approx 17/7$  per  $100 \text{ fb}^{-1}$ , to be compared with their best result  $S/B = 13/6$ <sup>2</sup> (for a discussion of the differences, see Section 7).

In Section 3 we proposed a new variable  $R_{p_T}$  that gives a direct signature of a hard  $W_L W_L$  scattering process and that replaces the conventional cuts. We thus now go back to the point where only generation level cuts and  $t\bar{t}$  cuts have been applied and study the correlations between the transverse momenta of the  $W$  bosons and the jets for those signal and background events which survived those cuts. This is shown in Fig. 10(a,b). It is apparent that a line corresponding to a constant ratio

$$p_T^{W_1}/p_T^{j_1} \cdot p_T^{W_2}/p_T^{j_2} = 12 \quad (10)$$

has indeed a large discriminating power between signal and background, leaving the bulk of the background above, while keeping a substantial part of the signal below. In Fig. 10(c) the same correlations are shown for the transverse momenta of the outgoing leptons instead of the  $W$ 's. Although  $W$  decay tends to smear this nice picture out (it is

<sup>2</sup>To derive this number, we take the row corresponding to  $M_{cut} = 400 \text{ GeV}$  from Table 4 of Ref. [5], treat the “ $M_H = 200 \text{ GeV}$ ” cross section as the irreducible background and subtract it from the “no Higgs” cross section to get the signal, then normalize the result to  $100 \text{ fb}^{-1}$ .



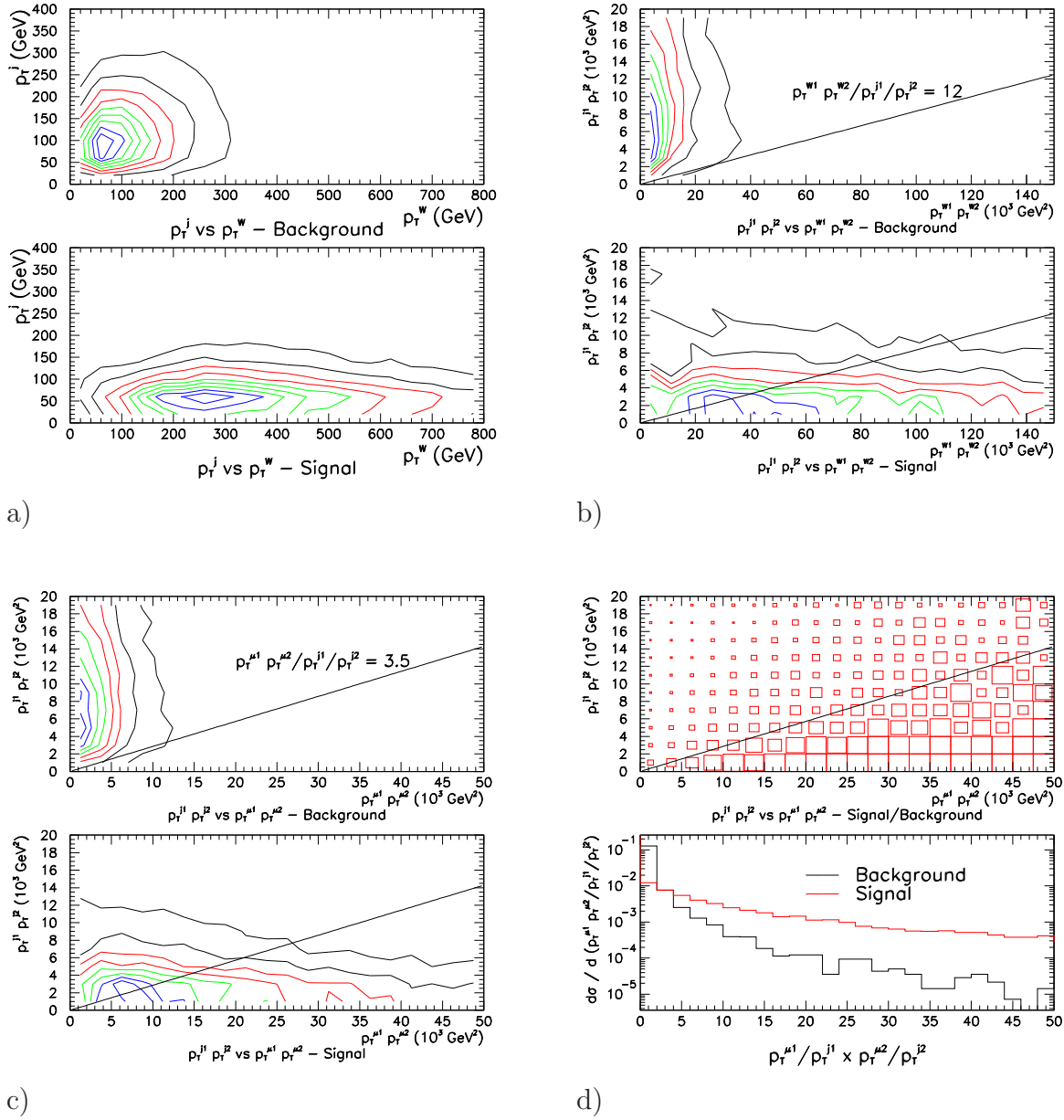


Figure 10: Transverse momenta and their combinations for signal and for the irreducible background in the  $jjW^+W^+$  channel at 14 TeV, after applying the cuts against top production: a) individual  $p_T$  of  $W$ 's and jets, b)  $p_T$  products of two  $W$ 's and two jets, c)  $p_T$  products of two leptons and two jets, and d) the signal to background ratio (top) and the  $R_{p_T}$  distribution for the signal and for the background (bottom). Contours in (a) through (c) represent the lines of constant cross section.

of course very important to take proper account of the correct angular distributions of  $W$  decays accordingly to the different helicities in signal and background, but these differences unfortunately do not play any positive role in isolating signal from background), the interesting observation is that the outgoing leptons from  $W$  decay sufficiently keep the basic kinematic features characteristic for signal and background of their parent  $W$ 's. Consequently, a line of constant ratio

$$R_{p_T} = 3.5 \tag{11}$$

still has a remarkably large discriminating power between signal and background. This is illustrated in Fig. 10(d), where the upper plot shows the ratio of signal to background and in the lower plot the  $R_{p_T}$  distributions for signal and background are given. When applied on top of all the remaining selection criteria, the efficiency of a cut that requires  $R_{p_T}$  be larger than 3.5 is 0.77 for the signal and 0.14 for the background, which makes it more effective than all the alternative conventional cuts taken together.

Thus, our complete set of selection criteria is now (set II):

- 2 same sign leptons,
- 2 tag jets with  $2 < |\eta_j| < 5$  and opposite directions,
- no  $b$ -tag,
- $M_{j_1 l_2}, M_{j_2 l_1} > 200$  GeV,
- $M_{jj} > 500$  GeV,
- $R_{p_T} > 3.5$ ,
- $\Delta\phi_{ll} > 2.5$ ,

Note that a combination of only the last two cuts allows to release several other selection criteria that are conventionally used to cope with the irreducible background. The  $R_{p_T}$  cut also automatically removes the  $t\bar{t}$  background related to leptonic  $B$  decay to a negligible level, hence we are free to drop any lepton isolation or central jet veto cut, which may well prove an advantage in a high pile-up regime like the LHC. Here we have also modified the  $M_{jj}$  cut to a higher value, since we find such change produce an improvement in combination with the  $R_{p_T}$  cut, but not in combination with the conventional cuts.

A summary of results obtained with the conventional cuts (set I) and the  $R_{p_T}$  cut (set II) is shown in Tables 1 and 2. For an easy comparison of both results, the selection criteria were chosen such as to keep in both cases a similar amount of signal. Relative to the amount of signal, we find the  $R_{p_T}$  cut improve rejection power against the irreducible background by a factor 2.5, and against the  $t\bar{t}$  background by about 1/3. Fig. 11(a) and (b) show the corresponding invariant mass distributions of the two same-sign leptons for this case (to be compared with respective plots in Fig. 9). We arrive at  $S/B \approx 12/4$  once all the  $l^+l^+$  channels are summed up and  $S/B \approx 14/6$  by additionally including the  $l^-l^-$  channels.

It is interesting to note that  $R_{p_T}$  being a dimensionless number does not depend on  $\sqrt{s}$  to first approximation. In principle, exactly the same cut could be also used in an

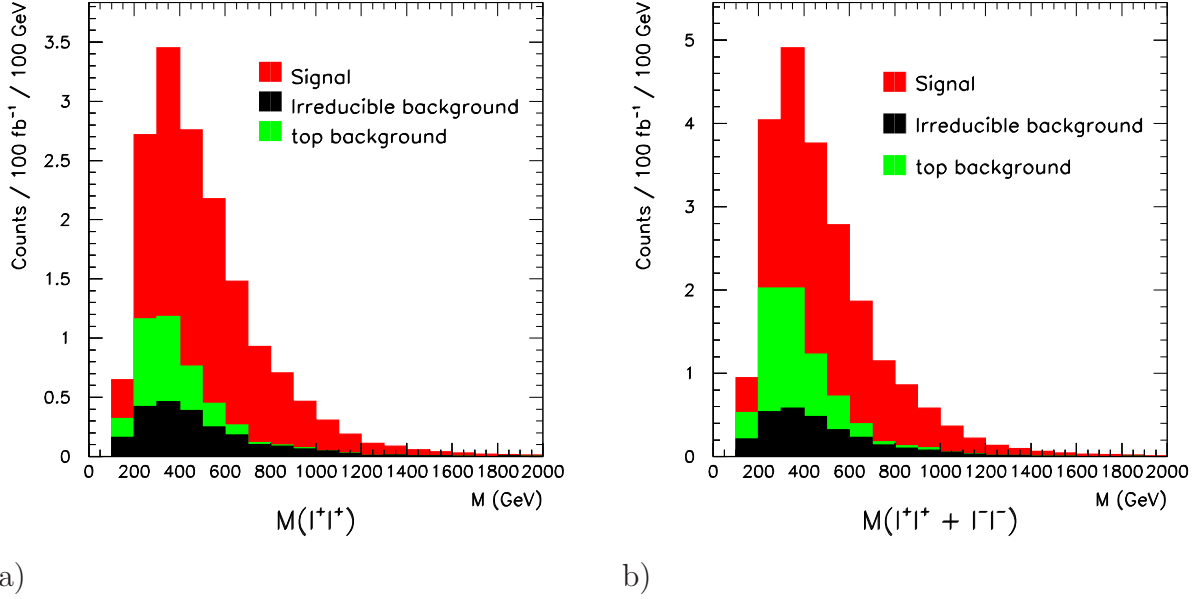


Figure 11: Invariant mass distributions of two same-sign leptons after all the new signal selection criteria (set II), normalized to  $100 \text{ fb}^{-1}$ : (a)  $jjl^+l^+$ , (b)  $jjl^+l^+$  and  $jjl^-l^-$  added.

Sample	Initial $\sigma$	Generated events	Selected evts (I)	Selected evts (II)	Other reductions	Final $\sigma$ (I)	Final $\sigma$ (II)
$W_L^+W_L^+$ SM	7.6 fb	56485	534	523	0.0426	0.0031 fb	0.0030 fb
$W_L^+W_L^+$ No Higgs	16.7 fb	56666	11903	12313	0.0335 (I)/0.0329 (II)	0.1117 fb	0.1193 fb
Irr. background	104.5 fb	170183	1893	855	0.0426	0.0494 fb	0.0224 fb
$t\bar{t}$ background	-	15000000	1805	1318	0.00008	0.0225 fb	0.0171 fb

Table 1: Results of conventional selection criteria (I) and new selection criteria (II) for the  $jjl^+l^+$  channel. The signal is the result of subtracting the first row from the second row. “Other reductions” stand for losses due to  $b$  tagging, lepton reconstruction and sign matching, respective branching fractions and the unitarity bound, wherever appropriate.

Sample	Initial $\sigma$	Generated events	Selected evts (I)	Selected evts (II)	Other reductions	Final $\sigma$ (I)	Final $\sigma$ (II)
$W_L^-W_L^-$ SM	1.72 fb	9078	93	94	0.0426	0.0008 fb	0.0008 fb
$W_L^-W_L^-$ No Higgs	4.30 fb	9298	1579	1747	0.0360 (I)/0.0357 (II)	0.0263 fb	0.0288 fb
Irr. background	20.35 fb	35615	525	241	0.0426	0.0128 fb	0.0059 fb
$t\bar{t}$ background	-	15000000	1805	1318	0.00008	0.0225 fb	0.0171 fb

Table 2: Results of conventional selection criteria (I) and new selection criteria (II) for the  $jjl^-l^-$  channel. The signal is the result of subtracting the first row from the second row. “Other reductions” stand for losses due to  $b$  tagging, lepton reconstruction and sign matching, respective branching fractions and the unitarity bound, wherever appropriate.

analysis of  $pp$  data at 7 TeV or at 8 TeV. The efficiency of such cut (calculated on top of all the other cuts) at  $\sqrt{s} = 7$  TeV (8 TeV) is 0.71 (0.72) for the signal and 0.12 (0.12) for the irreducible background, which is only slightly weaker than for  $\sqrt{s} = 14$  TeV. It is mainly due to the much lower signal cross section to begin with (factor  $\sim 7$  at the level of generation cuts) that 7 or 8 TeV ultimately does not offer the possibility to observe the signal in a viable amount of time. However, the efficiency of the  $R_{p_T}$  variable can be experimentally tested at 7 or 8 TeV.

## 6 The opposite-sign $WW$ channel

As already stated in Section 3, due to the many additional contributions to the background in the  $jjW^+W^-$  channel (both in terms of Feynman diagrams and physical processes), there is good reason to expect a lower  $R_{p_T}$  efficiency. In this Section we present our own analysis of the  $jjW^+W^-$  channel for the sake of a direct comparison. Generated samples, initial and final cross sections for the signal and for the backgrounds are shown in Table 3. Cuts imposed at the generation level were:

- $|\eta_j| < 5$ ,
- $\Delta\eta_{jj} > 4$ ,
- $p_T^j > 10$  GeV,
- $M_{jj} > 350$  GeV.

An attempt to exploit the kinematic correlations between  $W$ 's and jets and between leptons and jets, in a similar manner as was applied for the same-sign channel and presented in Section 5, is shown in Fig. 12. Many important differences with respect to the same-sign channel are readily visible. First and foremost, background extends to much lower jet transverse momenta, to the effect of background and signal being marginally distinguishable in the jet  $p_T$  distributions (Figs. 12(a) and (b)). In these circumstances, the  $R_{p_T}$  ratio can only be as effective in separating signal from background as lepton transverse momenta on their own. Fig. 12(d) confirms that no particular cut on  $R_{p_T}$  can bring background levels below or even close to the signal level without risking very low efficiency. This study concludes that  $R_{p_T}$  cannot be used as an effective discriminant. Larger initial cross sections for the signal are unfortunately coupled with a weaker kinematic separation from the background in  $p_T^l$  (see Fig. 12(c)). However, we find the sum  $p_T^{l_1} + p_T^{l_2}$  or the product  $p_T^{l_1} \cdot p_T^{l_2}$  still have a slightly larger efficiency than combined cuts on the individual  $p_T^l$ . Another important disadvantage is that top production can directly fake the signal signature here, rather than being restricted to small experimental effects, and an additional central jet veto is necessary to bring this background down to a manageable level. A veto on additional jets with  $p_T > 25$  GeV and  $\eta$  anywhere between  $\eta_{j1}$  and  $\eta_{j2}$  removes nearly 75% of the surviving  $t\bar{t}$  events at the expense of an additional 15% of the signal.

As usual, we require no tagged  $b$  and no additional leptons with  $p_T > 10$  GeV within  $|\eta| < 2$ . Finally, our full selection criteria are:

- exactly 2 opposite sign leptons within detector acceptance,

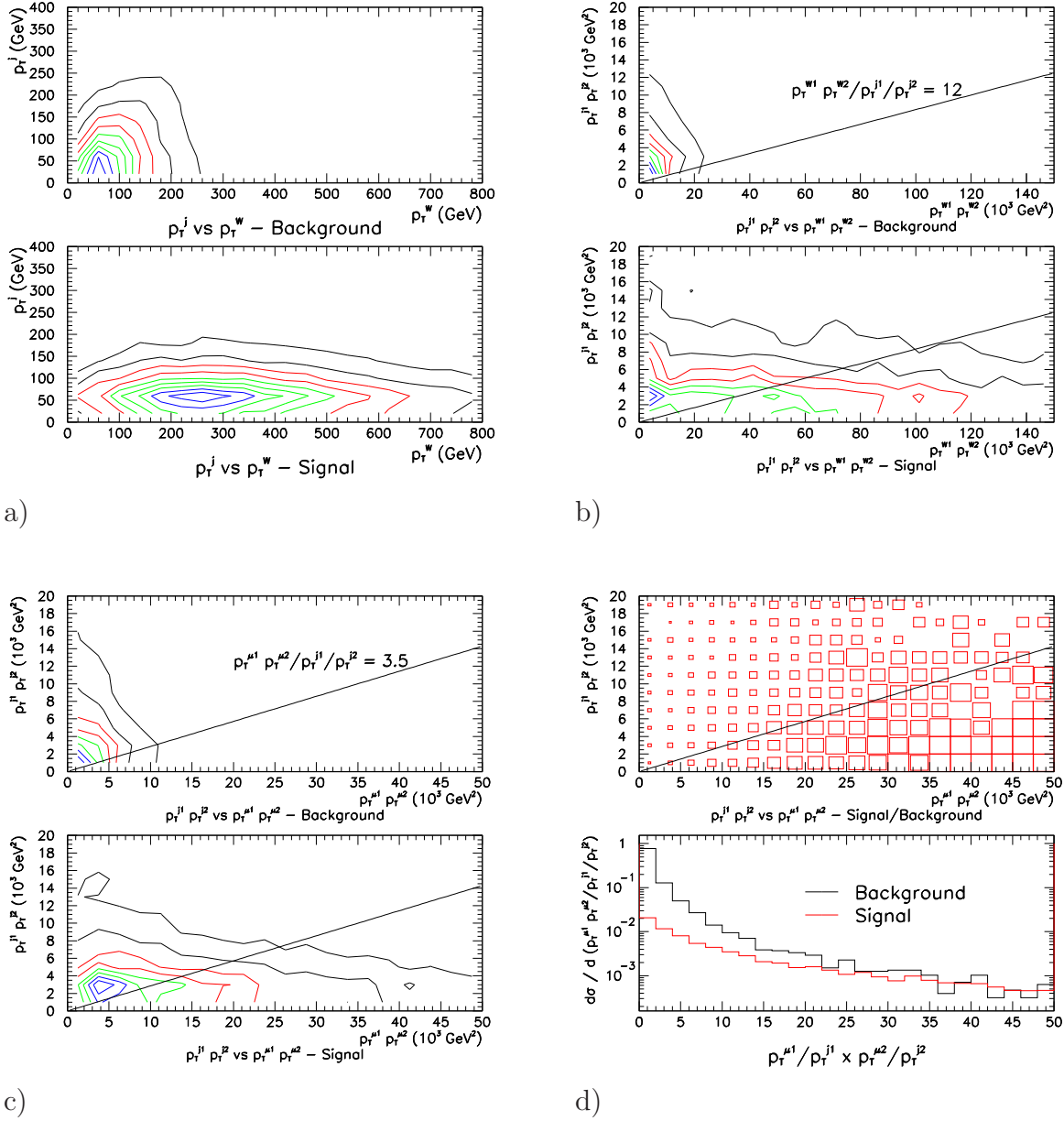


Figure 12: Transverse momenta and their combinations for signal and for the irreducible background in the  $jjW^+W^-$  channel at 14 TeV, after applying the cuts against top production: a) individual  $p_T$  of  $W$ 's and jets, b)  $p_T$  products of two  $W$ 's and two jets, c)  $p_T$  products of two leptons and two jets, and d) the signal to background ratio (top) and the  $R_{p_T}$  distribution for the signal and for the background (bottom). Contours in (a) through (c) represent the lines of constant cross section.

- 2 tag jets with  $2 < |\eta_j| < 5$  and opposite directions,
- no  $b$ -tag,
- $M_{j_1 l_2}, M_{j_2 l_1} > 200$  GeV,
- $M_{jj} > 500$  GeV,
- central jet veto,
- $p_T^{l_1} + p_T^{l_2} > 300$  GeV,
- $\Delta\phi_{ll} > 2.5$ ,
- $M_{ll} > 300$  GeV.

Sample	Initial $\sigma$	Generated events	Selected events	Other reductions	Final $\sigma$
$W_L^+ W_L^-$ EW SM	24.9 fb	90296	777	0.0426	0.0091 fb
$W_L^+ W_L^-$ EW No Higgs	44.0 fb	102570	8257	0.0362	0.1282 fb
Irr. background	3.37 pb	500000	458	0.0426	0.1315 fb
$t\bar{t}$ background	-	15000000	194	0.0028	0.3610 fb

Table 3: Results for the  $jjl^+l^-$  channel. The signal is the result of subtracting the first row from the second row. “Other reductions” stand for losses due to  $b$  tagging, lepton reconstruction, respective branching fractions and the unitarity bound, wherever appropriate.

The result (see Table 3) is consistent with those of previously published analyses on the same channel [5, 7] (taking into account all the differences in the respective analysis approaches), but does not bring much improvement to the subject.

## 7 Discussion and outlook

We have presented a detailed phenomenological analysis of  $WW$  scattering at the LHC, which in some aspects contains improvements with respect to the analyses published by other authors. Our analysis was optimized primarily for the discriminating power between alternative scenarios of EWSB and unitarity violation. The discrimination is based essentially on a counting experiment in which a light SM-like Higgs boson as the only source of EWSB should ideally produce an almost null result.

It is not the aim of this work to fine tune the selection in order to produce the best possible  $S/B$ , as the exact criteria will change anyway once a full detector simulation is included. Regardless of that it seems clear that the  $R_{p_T}$  variable is able to provide some new insight into the subject and possibly improve the expected performance in the same-sign  $WW$  channel. Our result with conventional cuts is roughly consistent with previously published results of similar analyses, in particular with the recent Ref. [5], if the same conditions and assumptions are applied in both cases. Their best result  $S/B = 13/6$  is

the equivalent of our  $S/B \approx 17/7$  per  $100 \text{ fb}^{-1}$ . In fact, most of the difference comes from the fact that their analysis includes a cut on the minimum jet  $p_T$  at 30 GeV which is the standard in LHC experiments, but very costly to the signal as far as  $W_L W_L$  selection at high invariant mass is concerned. With the  $R_{p_T}$  cut instead this result could become even  $S/B \approx 17/3$ .

The question of a practical minimum jet  $p_T$  cut, in particular having in view the large LHC pile-up, is an issue that requires a careful dedicated study which is clearly beyond the scope of the present work. In this paper we show a strong physics motivation for releasing the stringent cuts on jet  $p_T$  (our analysis implicitly assumes  $p_T > 10$  GeV, i.e., jets below that threshold are not reconstructed). The idea of tagging only one forward jet with  $p_T > 30$  GeV, which should be rather safe, and working out additional criteria to indentify correctly its softer companion, is an interesting possibility that needs to be investigated. Data collected in 2012 may already shed some light on the issue.

Our new selection criterion provides potential to improve the final figure of merit regardless of any working assumptions or approximations we have done throughout this paper. It is clear, however, that many important unknowns still remain and will require a careful experimental study. One is the vulnerability of  $R_{p_T}$  to experimental smearing in the measurement of all the individual  $p_T$ 's. Since  $R_{p_T}$  is expected to work for 7 or 8 TeV nearly as efficiently as for 14 TeV, the practical effects of  $p_T$  smearing can be studied at the LHC on 2012 data and reasonably assumed not to be worse for future 14 TeV data.

Top background poses more unknowns. The total cross section for top production at 14 TeV will ultimately have to be measured. Since  $t\bar{t}$  background to the  $W^+W^+$  channel arising from lepton sign misidentification is not completely negligible, the practical profits from using the  $R_{p_T}$  variable will depend on precise knowledge of the sign matching efficiencies of the individual detectors (for demonstration purposes we could of course tune the selection so to kill  $t\bar{t}$  completely, but such procedure would also end up in very low signal and hence is of little practical interest). One should note that an important cross check of the  $t\bar{t}$  background evaluation can be obtained by comparing the results of the two in principle separate measurements that this analysis involves: the  $j j l^+ l^+$  channel and the  $j j l^- l^-$  channel. Since the relative amounts of  $WW$  in the two channels are like 4:1 and the amounts of  $t\bar{t}$  like 1:1, the actual ratio will shed some light on the true composition of the sample. With enough data having been collected, the  $j j l^- l^-$  channel could be even used to estimate the remaining  $t\bar{t}$  background and subtract it.

Certainly it will be crucial to include the electron channels in addition to the experimentally purest muon channels, as the latter alone do not guarantee enough statistical significance. A further, more detailed, study based on a full detector simulation and detector-specific event reconstruction is vital for the good understanding of rejection capabilities of the detector backgrounds and the resulting purity of electron reconstruction.

Overall, results presented in this paper show that there is good chance to get some important hints about the mechanism of electroweak symmetry breaking already after the first  $100 \text{ fb}^{-1}$  of data at 14 TeV, by focusing on the purely leptonic  $W$  decay channels. We advocate the importance of the same-sign  $WW$  channel as the most promising one, particularly in the absence of low mass resonances (1-2 TeV) in the  $W^+W^-$  channel.

## Acknowledgments

This work has been supported in part by the Polish Ministry of Science and Higher Education as research projects 666/N-CERN/2010/0, N N202 230337 (2009-12) and N N202 103838 (2010-12) and by the Collaborative Research Center SFB676/1-2006 of the DFG.

## References

- [1] G. F. Giudice, C. Grojean, A. Pomarol, R. Rattazzi, JHEP **0706** (2007) 045 [arXiv:hep-ph/0703164].  
K. Cheung, C.-W. Chiang, T.-Ch. Yuan, Phys. Rev. **D78** (2008) 051701 [arXiv:0803.2661 [hep-ph]]  
and references therein.
- [2] J. Bagger, V. Barger, K. Cheung, J. Gunion, T. Han, G. A. Ladinsky, R. Rosenfeld, C. P. Yuan, Phys. Rev. **D49** (1994) 1246; Phys. Rev. **D52**, (1995) 3878.
- [3] A. Dobado, M. J. Herrero, J. R. Pelaez, E. Ruiz Morales, M. T. Urdiales, Phys. Lett. **B352** (1995) 400; Phys. Rev. **D62** (2000) 055011.  
J. M. Butterworth, B. E. Cox, J. R. Forshaw, Phys. Rev. **D65** (2002) 096014.  
A. Alboteanu, W. Kilian and J. Reuter, JHEP **0811**, 010 (2008) [arXiv:0806.4145 [hep-ph]].  
M. S. Chanowitz, W. B. Kilgore, Phys. Lett. **B322** (1994) 147; Phys. Lett. **B347** (1995) 387.
- [4] E. Accomando, A. Ballestrero, S. Bolognesi, E. Maina, C. Mariotti, JHEP **0603** (2006) 093, [arXiv:hep-ph/0512219].  
A. Ballestrero, G. Bevilacqua and E. Maina, JHEP **0905**, 015 (2009), [arXiv:0812.5084 [hep-ph]].  
A. Ballestrero, G. Bevilacqua, D. B. Franzosi and E. Maina, JHEP **0911**, 126 (2009) [arXiv:0909.3838 [hep-ph]].
- [5] A. Ballestrero, D. B. Franzosi, E. Maina, JHEP **1106** (2011) 013 [arXiv:1011.1514 [hep-ph]].
- [6] B. Jäger, C. Oleari and D. Zeppenfeld, JHEP **0607** (2006) 015 [hep-ph/0603177]; Phys. Rev. D **80**, 034022 (2009) [arXiv:0907.0580 [hep-ph]].
- [7] C. Englert, B. Jäger, M. Worek, D. Zeppenfeld, Phys. Rev. **D80** (2009) 035027 [arXiv:0810.4861 [hep-ph]].
- [8] B. Jäger and G. Zanderighi, JHEP **1111**, 055 (2011) [arXiv:1108.0864 [hep-ph]].  
T. Melia, P. Nason, R. Rontsch and G. Zanderighi, JHEP **1111**, 078 (2011) [arXiv:1107.5051 [hep-ph]].  
T. Melia, K. Melnikov, R. Rontsch and G. Zanderighi, Phys. Rev. D **83**, 114043 (2011) [arXiv:1104.2327 [hep-ph]].  
T. Melia, P. Nason, R. Rontsch and G. Zanderighi, Eur. Phys. J. C **71**, 1670 (2011)



- [arXiv:1102.4846 [hep-ph]].  
T. Melia, K. Melnikov, R. Rontsch and G. Zanderighi, JHEP **1012**, 053 (2010)  
[arXiv:1007.5313 [hep-ph]].
- [9] T. Han, D. Krohn, L.-T. Wang and W. Zhu, JHEP **1003** (2010) 082 [arXiv:0911.3656 [hep-ph]].
- [10] The ATLAS Collaboration, “Expected Performance of the ATLAS Experiment”, arXiv:0901.0512v4 (CERN-OPEN-2008-020).
- [11] N. Amapane *et al.*, CMS Analysis Note, CMS AN-2007/005.
- [12] R. Contino, Ch. Grojean, M. Moretti, F. Piccinini, R. Rattazzi, JHEP **1005** (2010) 089 [arXiv:1002.1011 [hep-ph]]  
A. Ballestrero, D. Buarque Franzosi, L. Oggero and E. Maina, arXiv:1112.1171 [hep-ph].
- [13] J. Alwall, M. Herquet, F. Maltoni, O. Mattelaer, T. Stelzer, JHEP **1106** (2011) 128 [arXiv:1106.0522 [hep-ph]].
- [14] R. N. Cahn and S. Dawson, Phys. Lett. B **136**, 196 (1984) [Erratum-ibid. B **138**, 464 (1984)].  
S. Dawson, Nucl. Phys. **B249** (1985) 42.  
G. L. Kane, W. W. Repko and W. B. Rolnick, Phys. Lett. B **148** (1984) 367.
- [15] T. Sjöstrand, S. Mrenna, P. Skands, JHEP **05** (2006) 026.
- [16] A. Ballestrero, A. Belhouari, G. Bevilacqua, V. Kashkan and E. Maina, Comput. Phys. Commun. **180** (2009) 401 [arXiv:0801.3359 [hep-ph]].
- [17] S. Dawson, Phys. Lett. B **217** (1989) 347.
- [18] CMS Collaboration, Phys. Lett. **B695**, 424 (2011),  
ATLAS Collaboration, arXiv:1108.3699 (CERN-PH-EP-2011-103), arXiv:1108.6273
- [19] CMS Collaboration, CMS Physics Analysis Summary, CMS PAS BTV-09-001
- [20] CMS Collaboration, JINST 5 T03022 (2010)
- [21] W. Adam *et al.*, CMS Analysis Note, CMS AN-2009/164
- [22] B. Zhu, P. Govoni, Y. Mao, C. Mariotti, W. Wu, Eur. Phys. J. **C71** (2011) 1514, arXiv:1010.5848 [hep-ex].